

Inhomogeneous Ballistic Aggregation

L. Frachebourg,¹ V. Jacquemet,¹ and Ph. A. Martin¹

Received February 5, 2001; revised June 25, 2001

The one-dimensional ballistic aggregation process is considered when the initial mass density or the initial particle velocities vanish outside of a finite or semi-infinite interval. In all cases, we compute the mass distributions in closed analytical form and study their long time asymptotics. The relevant length scales are found different (of the order t , $t^{2/3}$, $t^{1/2}$) if, at the initial time, particles occupy a finite (or semi-infinite) interval and if a finite (or infinite) number of them are set into motion.

KEY WORDS: Statistical mechanics; non equilibrium; adhesive dynamics; density profile.

1. INTRODUCTION

The one-dimensional ballistic aggregation process consists in a system of point particles, moving on a line and forming aggregates through perfectly inelastic, adhesive collisions. The motion between collisions is free. In binary collisions two particles merge instantaneously into a single aggregate with conservation of mass and momentum, but dissipation of energy. This dynamic is deterministic, randomness occurs only through the distribution of initial data.

From the viewpoint of the statistical mechanics of point particles, this model has been first introduced and studied numerically in ref. 1. However, in the context of fluid dynamics, it has been realized much earlier that the evolution of shock waves in the inviscid limit of the one-dimensional Burgers equation obeys the laws of ballistic aggregation (see refs. 2 and 3 and the books of refs. 4 and 5 for more background). Let us mention here that the motion of shock waves or its equivalent formulation in terms of

¹Institut de Physique Théorique, École Polytechnique Fédérale de Lausanne (EPFL), CH-1015 Lausanne, Switzerland.

adhesion dynamics has been proposed by Zeldovich as a model for investigating the large-scale structure of the universe.⁽⁶⁾ The Burgers equation is also relevant to the problem of surface growth via the deposition process,⁽⁷⁾ as well as to the dynamics of the exclusion particle system.⁽⁸⁾ An attractive feature of one-dimensional adhesion dynamics, in addition to its close connection to problems of various physical origins, is that it provides a mathematically tractable many-particle dynamic system.

In the previous works^(9,10) (see also ref. 11 for a short review), ballistic aggregation has been solved in closed analytical form when the distribution of initial data is homogeneous in space. In this homogeneous process, the mass density ρ of initial particles is uniform over the whole real line, all having the same mass m . Their initial momenta are uncorrelated, each of them being distributed according to the same Maxwellian

$$\varphi_m(p) = \left(\frac{\beta}{2\pi m} \right)^{1/2} \exp \left(-\frac{\beta p^2}{2m} \right) \quad (1)$$

where β is an inverse temperature.

In the present paper we consider various types of inhomogeneous processes. Inhomogeneity can stem in particular from a non uniform initial mass density $\rho(x)$, as well as from a non spatially constant initial temperature $\beta^{-1}(x)$. Physically, in a gas with elastic collisions, density and temperature gradients generate diffusive flows of particles. It is of interest to investigate the nature of such diffusion processes when the collisions are dissipative. Moreover, in relation with the Burgers equation, an inhomogeneous initial velocity distribution of the aggregating particles corresponds to non-uniform excitations of the initial Burgers field. More comments on this point are given in the concluding remarks.

Specifically, we treat the following cases:

(i) The initial mass density is constant in the finite interval $[0, \rho^{-1}M_0]$ or in the semi-infinite interval $[0, \infty)$ and equal to zero otherwise. All particles have the same temperature $\beta^{-1} > 0$.

In the course of time the particles will leak out of the interval where they are initially confined, still undergoing inelastic collisions. It transpires that the diffusion process obeys different scaling laws depending whether the total amount of mass is finite or infinite.

(ii) The initial mass density is constant on the whole line. The initial particles have the temperature $\beta^{-1} > 0$ in the finite interval $[0, \rho^{-1}M_0]$ or in the semi-infinite interval $[0, \infty)$ and are at rest elsewhere (i.e., at zero temperature).

In this case the inertia of particles at rest hinder the flow of the moving particles and we obtain still other scaling regimes.

We refer to case (i) as ballistic aggregation in empty space and to case (ii) as ballistic aggregation with particles at rest. The set of particles that have a non zero initial temperature will be called the set of (initially) excited particles.

The basic quantity to be studied in this paper is the probability density $\pi(x, M, t)$ for finding (in the continuum limit) an amount M of mass of the excited particles to the left of x at time t . Related to this quantity is the total average mass $\mathcal{M}(x, t)$ of excited particles found left of x

$$\mathcal{M}(x, t) = \int_0^{M_0} dM M \pi(x, M, t) = \int_{-\infty}^x dy \rho(y, t) \quad (2)$$

yielding the average mass density

$$\rho(x, t) = \frac{d}{dx} \mathcal{M}(x, t) \quad (3)$$

We emphasize that in all cases this mass density profile is obtained explicitly, a rather rare instance in the theory of inhomogeneous non-equilibrium systems.

Of interest will be the large time behavior of the distribution $\pi(\xi t^\alpha, M, t)$ when one looks at the system on various spatial scales $x = \xi t^\alpha$, $\alpha \geq 0$. In the homogeneous aggregation process, the only relevant scale is $x = \xi t^{2/3}$: typically, aggregates with masses of the order $M \sim t^{2/3}$ are found at distances $x \sim t^{2/3}$ from each other.^(1,9) Here, we determine the distribution $\pi(x, M, t)$ in closed analytical form for the cases (i) and (ii) described above. The finite interval case is treated in Section 2 and the semi-infinite interval in Section 3.

If the initial interval is finite and the particles aggregate in empty space, the large time scale will be ballistic, namely $x = \xi t$. Indeed, since there is a finite amount of mass available, for large times one will observe a number of clusters that move freely without colliding anymore. These moving clusters will be found at a distance of order t from the origin and from each other (Section 2.1). We find that $\pi(\xi t, M, t)$ has a well defined limit as $t \rightarrow \infty$, expressible in terms of the incomplete Gamma function (Eq. (17)) and represented in Fig 2a. The corresponding mass density profile has a slow decay in terms of the scaling variable ξ (see (29))

$$\lim_{t \rightarrow \infty} \rho(\xi t, t) \sim \frac{1}{2\xi^3}, \quad \xi \rightarrow \infty \quad (4)$$

If aggregation starting from a finite interval takes place in an environment of particles at rest, the pertinent scale becomes $x = \xi \sqrt{t}$ as indicated in the elementary example presented in the introduction of ref. 9. In this example one analyses the motion of a single particle, which collects the mass of the particles at rest along its way. In general, escape of excited particles is slowed by the inertia of particles at rest, and as a result an aggregate of mass $M \sim \sqrt{t}$ is typically found at distance $x \sim \sqrt{t}$ from the origin (Section 2.2). We find here that $\pi(\xi \sqrt{t}, M, t)$ converges to the distribution given by Eq. (35) and illustrated in Fig. 2b. In contrast to (4), the mass density profile has now the very fast decay $\sim 2 \sqrt{\frac{M_0}{\pi}} |\xi| \exp(-\frac{\xi^4}{4M_0})$, $\xi \rightarrow \infty$ (Eq. (39)).

The situation is drastically different if initially excited particles extend over a semi-infinite interval on the right, acting as an infinite reservoir of mass and momentum (Section 3.1). The initial particles will “evaporate” in empty space on the left, and one will observe a whole spectrum of masses $M \sim t^{2(1-\alpha)}$, $2/3 \leq \alpha \leq 1$, on distances $x \sim t^\alpha$. More precisely, at scale $x = \xi t^{2/3}$ one recovers the typical scaling properties valid for the homogeneous process, namely $t^{2/3} \pi(\xi t^{2/3}, \mu t^{2/3}, t)$ is equal to a time-independent scaling function written with the help of Airy functions (see (47) and (48)). There is a non trivial mass density profile at this scale (Eq. (52)), plotted in Fig. 4. Moreover, it is interesting to note that there is another non trivial limiting distribution $\lim_{t \rightarrow \infty} \pi(\xi t, M, t)$ (Eq. (53)) obtained in the ballistic regime $x = \xi t$. It gives the distribution of forerunner particles with masses of order 1 that move freely in front of the profile without undergoing aggregation anymore. At intermediate scales $x = \xi t^\alpha$, $\alpha < 1$, more massive aggregates can be formed, caught by the flow of particles continuously coming from the right. The total average mass of these aggregates grows as (see (54))

$$\mathcal{M}(\xi t^\alpha) \sim \frac{t^{2(1-\alpha)}}{4\xi^2}, \quad t \rightarrow \infty \quad (5)$$

interpolating between masses of order 1 and $t^{2/3}$

If the left space contains particles at rest, we find again a definite scaling function at scale $x = \xi t^{2/3}$ (Eq. (58)) because mass and momentum are constantly supplied from the reservoir on the right (Section 3.2). This leads to the mass density profile given in Fig. 4. The difference with the previous case is that, because of the slowing down effect caused by the particles at rest, there is no propagation of particles at distances $x = \xi t^\alpha$, $\alpha > 2/3$.

2. INITIALLY EXCITED PARTICLES IN A FINITE INTERVAL

We specify the model in more details. The initial particles, of mass m , are located on the sites of the one-dimensional lattice $\{ka, k = \dots, -1, 0, 1, \dots\}$ with lattice spacing a . In the model with discrete initial masses, we will compute the probability $\Pi_m(x, j, t)$ to find j initially excited particles left of x at time t . Of course during the time evolution these initially excited particles can merge one with another or with particles at rest on their way. We will consider more precisely the probability density for finding an amount M of mass of these excited particles left of x in the continuum limit defined as

$$\pi(x, M, t) = \lim_{m \rightarrow 0} \frac{1}{m} \Pi_m(x, j, t) \quad (6)$$

where we let $a \rightarrow 0, m \rightarrow 0$ keeping $m/a = \rho$, $M = jm$ fixed, as well as $M_0 = Nm$ when we have a finite interval comprising N initially excited particles. In the rest of the paper the initial mass density ρ will be set equal to one for simplicity.

The whole analysis depends on the observation that an aggregate is moving along the trajectory of the center of mass of its constituting particles. Trajectories of center of mass are uniquely determined by initial positions and momenta. Let

$$X_{\ell+1}^r(t) = (2\ell + 1 + r) \frac{a}{2} + \frac{P_{\ell+1}^r t}{rm} \quad (7)$$

be the center of mass of the cluster of the r particles initially located at $\{(\ell+1)a, \dots, (\ell+r)a\}$ with total momentum $P_{\ell+1}^r = \sum_{k=1}^r p_{\ell+k}$. The initially excited particles may occupy the lattice sites $\{ka, k = 1, \dots, N\}$ ($N = M_0/m$) or the semi-infinite lattice $\{ka, k = 1, 2, \dots\}$. The necessary and sufficient condition to find j of them left of x at time t , $j = 0, 1, \dots, N$, is $X_{j+1}^r(t) > x$, $r = 1, 2, \dots$ and $X_{j+1-r}^r(t) < x$, $r = 1, 2, \dots$, namely all centers of mass of clusters of initial particles right of ja are found right of x at time t and those of clusters of initial particles left of ja (ja included) are found left of x (see ref. 9). Hence

$$\Pi_m(x, j, t) = \left\langle \prod_{r \geq 1} \theta(X_{j+1}^r(t) - x) \prod_{r \geq 1} \theta(x - X_{j+1-r}^r(t)) \right\rangle, \quad j = 0, 1, \dots \quad (8)$$

where the average is taken over the momentum distribution of the initial particles and θ is the Heaviside function. In the discrete model, this probability has obviously the normalization

$$\sum_{j \geq 0} \Pi_m(x, j, t) = 1 \quad (9)$$

since at any time either 0, 1, ... or all excited particles have to be found to the left of x .

2.1. Aggregation in Empty Space

The N initial particles occupy the sites ka , $k = 1, \dots, N$, with total mass $M = Nm$. Since initial particles have the independent momentum distribution (1), the probability (8) has a factorized form written as

$$\Pi_m(x, j, t) = J_m((j+1/2)a - x, j, t) J_m(x - (j+1/2)a, N-j, t) \quad (10)$$

with

$$\begin{aligned} J_m(Y, j, t) &= \left\langle \prod_{r=1}^j \theta(x - X_{j+1-r}^r(t)) \right\rangle \\ &= \int dP_1 \cdots \int dP_j \varphi_m(P_1) \cdots \varphi_m(P_j) \prod_{r=1}^j \theta(P_r - f_Y(rm, t)) \end{aligned} \quad (11)$$

where the parabola

$$f_Y(y, t) = \frac{y}{t} \left(Y - \frac{y}{2} \right) \quad (12)$$

results of the constraints on the center of masses expressed in (8). The derivation is analogous to that found in ref. 9; $J_m(Y, j, t)$ can be interpreted as the measure of Brownian paths starting from the origin at "time" $y = 0$ and that must be above the parabola $f_Y(y, t)$ at discrete "times" $y_r = rm$, $r = 1, \dots, j$. This is illustrated in Fig. 1a.

We expect that the particles do not undergo collisions anymore for large times, so we set $x = \xi t$ and compute

$$\lim_{t \rightarrow \infty} \Pi_m(\xi t, j, t) \equiv \Pi_m^\infty(\xi, j) \quad (13)$$

which represents the distribution of mass that moves asymptotically freely left of ξt as $t \rightarrow \infty$. This is easily done by noting that with $Y = (j+1/2)a - \xi t$,

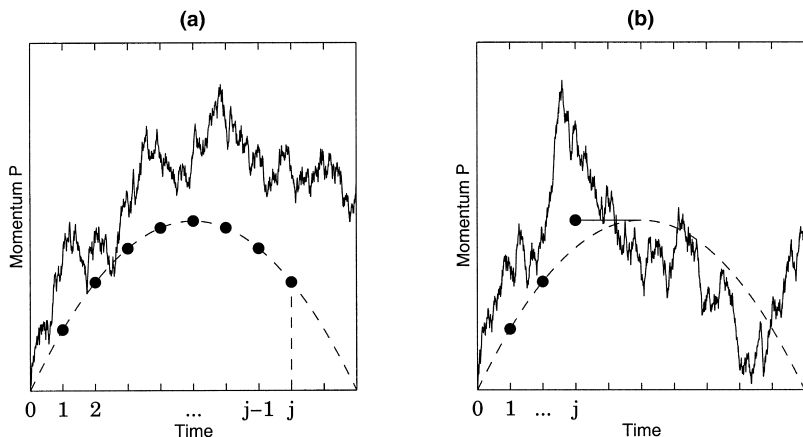


Fig. 1. The black dots represent the constraints on Brownian motion in Eq. (8), Fig. 1a, and in Eq. (29), Fig. 1b.

$\lim_{t \rightarrow \infty} f_Y(y, t) = -\xi y$ so the parabolic constraint reduces to a linear one, and the function $J_m(Y, j, t)$ tends to the measure $J_m^\infty(\xi, j)$ of Brownian paths starting from the origin and that must be above the linear barrier $-\xi y$ at discrete “times” $y_r = rm, r = 1, \dots, j$.

Next we evaluate from (13) the probability density for finding an amount of mass M left of ξt in the continuum limit.²

$$\pi^\infty(\xi, M) = \lim_{m \rightarrow 0} \frac{1}{m} \Pi^\infty(\xi, j) \tag{14}$$

For this we use for instance the result of the proposition in Section 8 of ref. 12,³ namely,

$$\begin{aligned} \lim_{m \rightarrow 0} \frac{1}{\sqrt{m}} J_m^\infty(\xi, j) &= \frac{1}{2} \int_{-\xi M}^\infty \frac{\partial}{\partial P_0} K_\xi(0, P_0, M, P)|_{P_0=0} dP \\ &\equiv J^\infty(\xi, M), \quad 0 < M < M_0 \end{aligned} \tag{15}$$

where $K_\xi(0, P_0, M, P)$ is the conditional measure of Brownian paths starting from P_0 at “time” 0, ending at P at “time” M and lying above the line

² Here we first take the long time limit followed by the continuum limit, but the order of these limits is irrelevant, see the remark after (22).

³ In this paper the parameters β and b in ref. 12 are set equal to $\beta = 2, b = 1$.

$-\xi M$ for all intermediate “times.” This kernel is recalled in Appendix A and a straightforward calculation leads to

$$J^\infty(\xi, M) = |\xi| \left(2\theta(\xi) + \frac{1}{2\sqrt{\pi}} \Gamma_{-1/2}(M\xi^2) \right), \quad 0 < M < M_0 \quad (16)$$

where $\Gamma_\nu(x) = \int_x^\infty dy e^{-y} y^{\nu-1}$ is the incomplete gamma function. Hence from (10)-(16) the final result is for $0 < M < M_0$

$$\begin{aligned} \pi^\infty(\xi, M) &= \frac{\xi^2}{\sqrt{\pi}} \Gamma_{-1/2}(M\xi^2) \left(1 + \frac{1}{4\sqrt{\pi}} \Gamma_{-1/2}((M_0 - M)\xi^2) \right), & \xi < 0 \\ \pi^\infty(\xi, M) &= \pi^\infty(-\xi, M_0 - M), & \xi > 0 \end{aligned} \quad (17)$$

Relation (15) only determines $\pi^\infty(\xi, M)$ for $M \neq \{0, M_0\}$ and one must still check if $\pi^\infty(\xi, M)$ carries a non zero finite weight at $M = 0$ and $M = M_0$ corresponding to a non zero probability for finding no mass or the total mass left of ξt as $t \rightarrow \infty$. To check this point we note that from (17) (see Appendix A)

$$\int_0^{M_0} dM \pi^\infty(\xi, M) = 1 \quad (18)$$

So $\{M: 0 \leq M \leq M_0\}$ is a set of measure equal to 1 and the determination of the asymptotic mass distribution (17) is thus complete.

Since

$$\Gamma_{-1/2}(M) \sim 2/\sqrt{M}, \quad M \rightarrow 0, \quad (19)$$

one sees that there is a strong enhancement of the probability density to find small aggregates left of ξt , $\xi < 0$,

$$\pi^\infty(\xi, M) \sim \frac{\xi^2}{\sqrt{M}} \left(\frac{2}{\sqrt{\pi}} + \frac{1}{2\pi} \Gamma_{-1/2}(M_0\xi^2) \right), \quad M \rightarrow 0, \quad \xi < 0 \quad (20)$$

As $\xi \rightarrow 0$, $\pi_\infty(\xi, M)$ tends to

$$\pi^\infty(0, M) = \frac{1}{\pi \sqrt{M(M_0 - M)}} \quad (21)$$

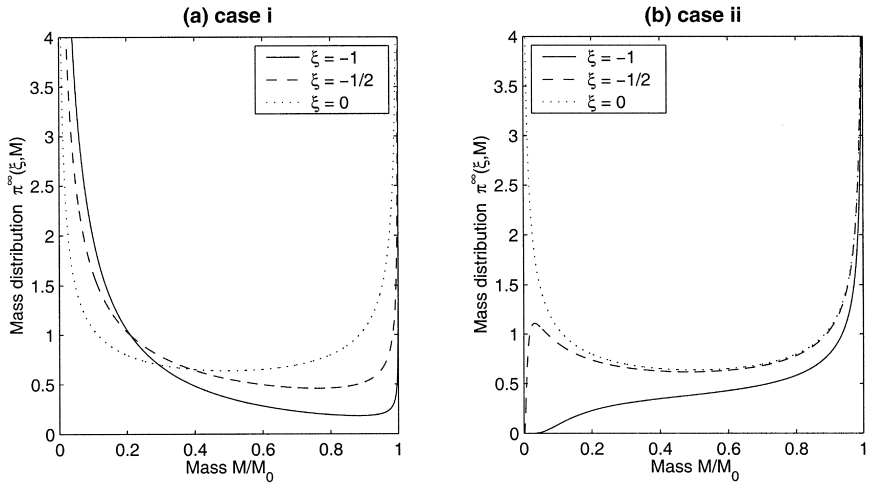


Fig. 2. Mass distribution Eq. (14) for aggregation in empty space (Fig. 2a), and Eq. (32) for aggregation with particles at rest (Fig. 2b). In the latter case, one must add the contribution $\delta(M) \tilde{\Pi}^\infty(\xi, 0)$ at $M = 0$.

showing a symmetric distribution of the mass around $M_0/2$. The distribution $\pi^\infty(\xi, M)$ as a function of M for various values of $\xi < 0$ is represented in Fig. 2a.

At this point we note that it is also possible to determine the probability density $\pi(x, M, t) = \lim_{m \rightarrow 0} \Pi_m(x, j, t)/m$ in the continuum limit for all times in an explicit form

$$\pi(x, M, t) = J(M - x, M, t) J(x - M, M_0 - M, t) \tag{22}$$

where the function $J(Y, M, t)$ (see Section 3.1) is given in Appendix B. Then one can check using the asymptotic properties of $J(Y, M, t)$ that $\lim_{t \rightarrow \infty} \pi(\xi t, M, t) = \pi^\infty(\xi, M)$ leads to the result (17) (this is sketched in Appendix B). Thus the large time asymptotics and the description in the continuum are exchangeable limits.

From (2) the total average mass $\mathcal{M}(\xi)$ found left of ξt as $t \rightarrow \infty$ for $\xi < 0$ is

$$\begin{aligned} \mathcal{M}^\infty(\xi) &= \lim_{t \rightarrow \infty} \mathcal{M}(\xi t, t) = \int_0^{M_0} dM M \pi^\infty(\xi, M) \\ &= \frac{1}{\sqrt{\pi} \xi^2} \int_0^{M_0 \xi^2} dM M \Gamma_{-1/2}(M) \\ &\quad + \frac{M_0}{8\pi} \int_0^{M_0 \xi^2} \Gamma_{-1/2}(M) \Gamma_{-1/2}(M_0 \xi^2 - M) \end{aligned} \tag{23}$$

and for $\xi > 0$,

$$\mathcal{M}^\infty(\xi) = M_0 - \mathcal{M}^\infty(-\xi) \quad (24)$$

Using (17), $\mathcal{M}_\infty(\xi)$ can be written in the alternative forms

$$\begin{aligned} \mathcal{M}^\infty(\xi) &= \frac{1}{\sqrt{\pi}} \int_0^{M_0 \xi^2} dM \Gamma_{-1/2}(M) \left(\frac{M}{\xi^2} - \frac{M_0}{2} \right) + \frac{M_0}{2} \\ &= \frac{1}{\sqrt{\pi} \xi^2} \int_0^{M_0 \xi^2} dM M \Gamma_{-1/2}(M) + \frac{M_0}{2} \int_0^{M_0 \xi^2} dM \Gamma_{-1/2}(M) \end{aligned} \quad (25)$$

The last line results from $\int_0^\infty dM \Gamma_{-1/2}(M) = \sqrt{\pi}$.

The asymptotic behaviors of $\mathcal{M}^\infty(\xi)$ as $|\xi| \rightarrow \infty$ or $|\xi| \rightarrow 0$ are easily found from the expressions in (25). For $\xi < 0$,

$$\mathcal{M}^\infty(\xi) \sim \frac{1}{4\xi^2}, \quad \xi \rightarrow -\infty \quad (26)$$

$$\sim \frac{M_0}{2} - \frac{2M_0^{3/2}}{3\sqrt{\pi}} |\xi|, \quad \xi \rightarrow 0, \quad \xi < 0 \quad (27)$$

In particular, $\mathcal{M}^\infty(0) = \frac{M_0}{2}$.

We deduce from the preceding results that the mass density profile $\rho(x, t)$ (2) has the scaling limit

$$\rho^\infty(\xi) = \lim_{t \rightarrow \infty} t \rho(\xi t, t) = \frac{d}{d\xi} \mathcal{M}_\infty(\xi) \quad (28)$$

and from (26)

$$\rho^\infty(\xi) \sim \frac{1}{2|\xi|^3}, \quad \xi \rightarrow \pm\infty \quad (29)$$

This profile represents the asymptotic average mass density of particles subjected to ballistic aggregation starting from a uniform distribution in a finite interval $[0, M_0]$. It is an even function of ξ and it is plotted in Fig. 3.

To conclude this section we remark that if one looks at distances that do not correspond to ballistic motion, i.e., $x = \xi t^\alpha$, $\alpha \geq 0$, $\alpha \neq 1$, one finds that with $Y = (j + 1/2) a - \xi t^\alpha$, $\xi < 0$, the constraint $f_Y(y, t)$ tends to ∞ or 0 depending if $\alpha > 1$ or $0 \leq \alpha < 1$, which is equivalent to $\xi \rightarrow -\infty$ or $\xi \rightarrow 0$.

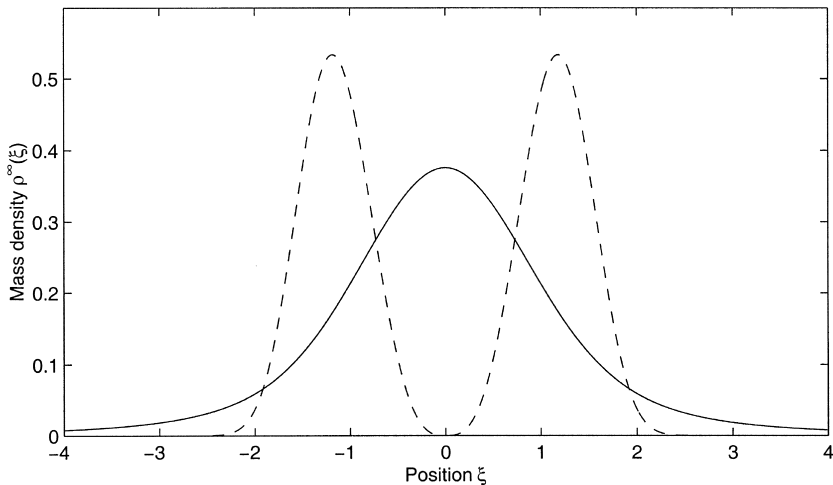


Fig. 3. The mass density for aggregation (finite excited interval): (i) in empty space at scale ξt (solid curve, Eq. (25)); (ii) with particles at rest at scale $\xi \sqrt{t}$ (dashed curve, Eq. (35)).

If $\alpha > 1$, $\lim_{\xi \rightarrow -\infty} \pi^\infty(\xi, M) = 0$ since no particle has a motion faster than ballistic. If $0 \leq \alpha < 1$ the limiting distribution is always $\pi^\infty(M, 0)$ given by (21). At all these scales and on the average the total mass splits asymptotically in equal parts to the left and to the right.

Our analysis does not give information on the statistics of the number of aggregates at large time as well as their individual masses. Nice results of this type are found in ref. 13. In particular the probabilities (for the discrete system) to have asymptotically exactly k aggregates or an aggregate of mass m_j are obtained for a general class of initial velocity distributions.

2.2. Aggregation with Particles at Rest

As in (10), the probability to find j initially excited particles left of x factorizes

$$\tilde{I}_m(x, j, t) = \tilde{J}_m((j+1/2) a - x, j, t) J_m(x - (j+1/2) a, N - j, t) \quad (30)$$

with

$$\begin{aligned} \tilde{J}_m(Y, j, t) = & \int dP_1 \cdots \int dP_j \varphi_m(P_1) \cdots \varphi_m(P_j) \\ & \times \prod_{r=1}^j \theta(P_r - f_Y(rm, t)) \prod_{r=j+1}^\infty \theta(P_j - f_Y(rm, t)) \end{aligned} \quad (31)$$

Here the additional constraints $\prod_{r=j+1}^{\infty} \theta(P_j - f_Y(rm, t))$ come from the conditions on the centers of mass of clusters involving initial particles at rest that can be set into motion through collisions with excited particles. Now if $x = (j + 1/2)a - Y < 0$, one has $\sup_{r>j} f_Y(rm, t) = Y^2/2t$ and if $x > 0$, $\sup_{r>j} f_Y(rm, t) = f_Y(jm, t)$. Hence for $x < 0$

$$\begin{aligned} \tilde{J}_m(Y, j, t) &= \int dP_1 \cdots \int dP_j \varphi_m(P_1) \cdots \varphi_m(P_j) \\ &\quad \times \prod_{r=1}^j \theta(P_r - f_Y(rm, t)) \theta\left(P_j - \frac{Y^2}{2t}\right) \end{aligned} \tag{32}$$

whereas $\tilde{J}_m(Y, j, t)$ reduces to $J_m(Y, j, t)$ Eq. (11) when $x > 0$. This is illustrated in Fig. 1b.

We introduce the scaling $x = \xi \sqrt{t}$. With $Y = (2j + 1)a - \xi \sqrt{t}$, one has $Y^2/2t \rightarrow \xi^2/2$ and $f_Y(y, t) \rightarrow 0$ as $t \rightarrow \infty$. Therefore, when $\xi < 0$, $\tilde{J}_m(Y, j, t)$ tends to the measure $\tilde{J}_m(\xi, j)$ of Brownian paths starting from the origin that are positive at discrete "times" $y_r = rm, r = 1, \dots, j - 1$, and surpass the point $\xi^2/2$ at "time" jm . In the continuum limit with $jm = M$

$$\begin{aligned} \lim_{m \rightarrow 0} \frac{1}{\sqrt{m}} \tilde{J}_m^\infty(\xi, j) &= \frac{1}{2} \int_{\xi^2}^{\infty} \frac{\partial}{\partial P_0} K(0, P_0, M, P)|_{P_0=0} dP \\ &\equiv \tilde{J}^\infty(\xi, M), \quad \xi < 0, \quad 0 < M < M_0 \end{aligned} \tag{33}$$

where $K_0(0, P_0, M, P)$ is the conditional measure of Brownian paths starting from P_0 at "time" 0, ending at P at "time" M and remaining positive for all intermediate "times." With the help of (60) and (61) the calculation leads to

$$\tilde{J}^\infty(\xi, M) = \frac{1}{\sqrt{\pi M}} \exp\left(-\frac{\xi^4}{4M}\right), \quad \xi < 0, \quad 0 < M < M_0 \tag{34}$$

When $\xi > 0$ and $x = \xi \sqrt{t}$, $f_Y(y, t) \rightarrow 0$ as $t \rightarrow \infty$, and in the continuum limit $\tilde{J}_m(Y, j, t)/\sqrt{m}$ reduces to $J^\infty(\xi = 0, M) = 1/\sqrt{\pi M}$ by (16) and (19). Hence, we have $\lim_{t \rightarrow \infty} \tilde{I}_m(\xi \sqrt{t}, j, t) = \tilde{I}_m^\infty(\xi, j)$ and

$$\begin{aligned} \tilde{\pi}^\infty(\xi, M) &= \lim_{m \rightarrow 0} \frac{1}{m} \tilde{I}_m^\infty(\xi, j) = \frac{1}{\pi \sqrt{M(M_0 - M)}} \exp\left(-\frac{\xi^4}{4M}\right), \quad \xi < 0 \\ \tilde{\pi}^\infty(\xi, M) &= \tilde{\pi}^\infty(-\xi, M_0 - M), \quad \xi > 0 \end{aligned} \tag{35}$$

This holds for $0 < M < M_0$. In order to check for normalization, we will use the equation [ref. 14, p. 366]

$$\int_u^\infty \frac{(x-u)^v}{x} e^{-\mu x} = u^v \Gamma(v+1) \Gamma_{-v}(u\mu)$$

we find from (35)

$$\int_0^{M_0} dM \tilde{\pi}^\infty(\xi, M) = \frac{1}{\sqrt{\pi}} \Gamma_{1/2}(\xi^4/M_0) \quad (36)$$

so that there is the probability

$$\tilde{\Pi}^\infty(\xi, 0) = 1 - \frac{1}{\sqrt{\pi}} \Gamma_{1/2}(\xi^4/M_0) = \frac{1}{\sqrt{\pi}} \gamma_{1/2}(\xi^4/M_0) \quad (37)$$

($\gamma_v(x) = \int_0^x dy e^{-y} y^{v-1}$) that no fraction of the initially excited particles is found left of $\xi \sqrt{t}$, $\xi < 0$, as $t \rightarrow \infty$. In Appendix A, we provide a direct calculation of the total amount M_0 of excited particles remaining on the right of $\xi \sqrt{t}$ which of course coincides with (37).⁴ Note that for $\xi = 0$, the distribution (35) reduces to the same form (21) found for aggregation in empty space. The distribution $\tilde{\pi}^\infty(\xi, M)$ as a function of M is shown in Fig. 2b for various values of ξ .

As before one can calculate the mass $\tilde{\mathcal{M}}^\infty(\xi) = \int_0^{M_0} dM M \tilde{\pi}^\infty(\xi, M)$ of initially excited particles left of $\xi \sqrt{t}$ as $t \rightarrow \infty$ and the mass density profile $\tilde{\rho}^\infty(\xi) = d\tilde{\mathcal{M}}^\infty(\xi)/d\xi$ at the scale $x = \xi \sqrt{t}$ with the result

$$\tilde{\rho}^\infty(\xi) = |\xi|^3 \frac{1}{\sqrt{\pi}} \Gamma_{1/2}(\xi^4/4M_0) \quad (38)$$

$$\sim 2 \sqrt{\frac{M_0}{\pi}} |\xi| \exp\left(-\frac{\xi^4}{4M_0}\right), \quad \xi \rightarrow \pm\infty \quad (39)$$

This decay is much faster than the behavior (29) found in the case of aggregation in empty space. This is of course due to the fact that the inertia of the particles at rest prevents a fast escape of the excited particles. Moreover, since the latter particles necessarily collect the mass of the particles at rest on a distance of the order $\xi \sqrt{t}$, the mass of the first aggregate

⁴ Then the full density probability has a $\delta(M) \Pi^\infty(\xi, 0)$ weight at the point $M = 0$, but this does not contribute to the mass density (39).

moving to the left (or to the right) grows as \sqrt{t} . This is represented in Fig. 3: the two peaks at $\pm \xi_0$ reflect indeed the fact that on the average we will observe a mass of order \sqrt{t} well localized around $\pm x_0 = \pm \xi_0 \sqrt{t}$.

Scalings $x = \xi t^\alpha$, $\xi < 0$ with $\alpha > 1/2$ or $0 \leq \alpha < 1/2$ correspond to the limiting cases $\xi \rightarrow -\infty$ or $\xi \rightarrow 0$. Thus the probability to find excited particles at scales larger than $\xi \sqrt{t}$ vanishes whereas it remains equal to the distribution (21) on scales shorter than $\xi \sqrt{t}$.

3. INITIALLY EXCITED PARTICLES IN A SEMI-INFINITE INTERVAL

3.1. Aggregation in Empty Space

The initial particles occupy the sites of the semi-infinite lattice $\{ka, k = 1, 2, \dots\}$. The probability to find j initially excited particles left of x is obtained by letting $N \rightarrow \infty$ in (10). This yields

$$\Pi_m(x, j, t) = J_m((j+1/2)a - x, j, t) J_m(x - (j+1/2)a, t) \quad (40)$$

where the function

$$J_m(Y, t) = \lim_{N \rightarrow \infty} J_m(Y, N, t) \quad (41)$$

is the same as that studied in refs. 10 and 11; it is the measure of Brownian paths starting from the origin constrained to be above the parabola $f_Y(y, t)$ for all discrete times $y_r = rm$, $r = 1, 2, \dots$. Now one has the normalization

$$\sum_{j=0}^{\infty} \Pi_m(x, j, t) = 1 \quad (42)$$

In the continuum limit the corresponding functions $J(Y, M, t)$ and $J(Y, t)$ are expressed in term of the conditional measure $K_f(0, P_0, M, P)$ of Brownian paths starting from P_0 at "time" 0, ending at P at "time" M and lying above the parabola $f_Y(y, t)$ for all "intermediate times":

$$J(Y, M, t) = \lim_{m \rightarrow 0} \frac{1}{\sqrt{m}} J_m(Y, j, t) = \frac{1}{2} \int_{f_Y(M, t)}^{\infty} dP \frac{\partial}{\partial P_0} K_f(0, P_0, M, P)|_{P_0=0} \quad (43)$$

$$J(Y, t) = \lim_{M \rightarrow \infty} J(Y, M, t)$$

The properties of these functions are described in the Appendix B. Thus the probability density to find an amount of mass $M > 0$ left of x at time t is given by

$$\pi(x, M, t) = \lim_{m \rightarrow 0} \frac{1}{m} \Pi_m(x, j, t) = J(M-x, M, t) J(x-M, t) \quad (44)$$

and it is normalized to one⁵

$$\int_0^\infty J(M-x, M, t) J(x-M, t) dx = 1 \quad (45)$$

In contrast to the finite interval case we can explicitly extract the time dependence by scaling:

$$\begin{aligned} J(Y, M, t) &= t^{-1/3} J(Yt^{-2/3}, Mt^{-2/3}) \\ J(Y, t) &= t^{-1/3} J(Yt^{-2/3}) \end{aligned} \quad (46)$$

where $J(Y, M)$ and $J(Y)$ are the above functions evaluated at $t = 1$.

By consequence, the time dependence of the probability density (44) is given by

$$\pi(M, x, t) = t^{-2/3} J(Mt^{-2/3} - xt^{-2/3}, Mt^{-2/3}) J(xt^{-2/3} - Mt^{-2/3}) \quad (47)$$

Hence the probability to find a mass M between $\mu t^{2/3}$ and $(\mu + d\mu) t^{2/3}$ left of $x = \xi t^{2/3}$ is $\pi(\mu, \xi) d\mu$ with

$$\pi(\xi, \mu) = J(\mu - \xi, \mu) J(\xi - \mu) \quad (48)$$

The average mass left of $\xi t^{2/3}$ is then

$$\begin{aligned} \mathcal{M}(\xi t^{2/3}, t) &= t^{2/3} \mathcal{M}(\xi) \\ \mathcal{M}(\xi) &= \int_0^\infty d\mu \mu J(\mu - \xi, \mu) J(\xi - \mu) \end{aligned} \quad (49)$$

⁵ It can be checked that the weight at the point $M = 0$ is zero as in the case of the finite interval.

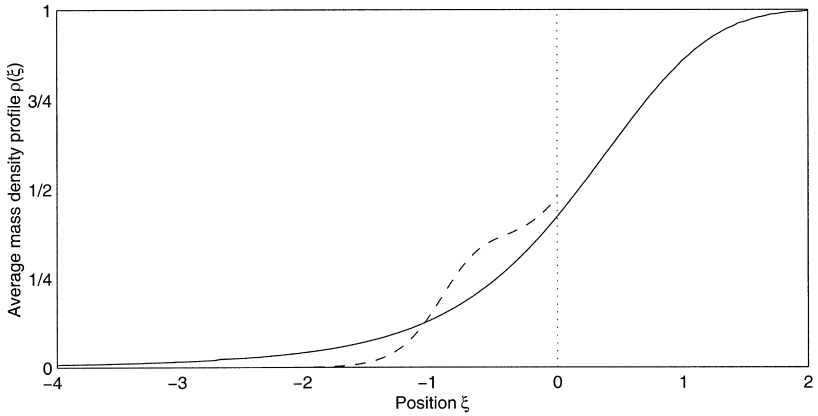


Fig. 4. The mass density for aggregation (semi-infinite excited interval) in empty space at scale $\xi t^{2/3}$ (solid curve, Eq. (49)). For aggregation with particles at rest, the mass density of excited particles is the dashed curve for $\xi < 0$. For $\xi > 0$, the curves are identical.

The asymptotic behavior of (49) as $\xi \rightarrow -\infty$ is obtained by inspection of functions $J(\mu - \xi, \mu)$ and $J(\xi - \mu)$ and found to be (Appendix B)

$$\mathcal{M}(\xi) \sim \frac{1}{4\xi^2}, \quad \xi \rightarrow -\infty \quad (50)$$

Hence the mass density profile $\rho(\xi) = \frac{d}{d\xi} \mathcal{M}(\xi)$ behaves as $\sim \frac{1}{2|\xi|^3}$, $\xi \rightarrow -\infty$ as in the finite interval problem, see (29). Writing (49) as

$$\mathcal{M}(\xi) = \int_{-\xi}^{\infty} d\mu (\mu + \xi) J(\mu, \mu + \xi) J(-\mu) \quad (51)$$

and using (45) and (70), $\rho(\xi)$ can be written in the form

$$\rho(\xi) = 1 - e^{-\xi^3/3} \int_0^{\infty} d\mu \mu \mathcal{F}(\mu) \mathcal{J}(\xi - \mu) \quad (52)$$

The functions \mathcal{F} and \mathcal{J} are defined in (67) and (70). Hence $\rho(\xi)$ saturates to its bulk value $\rho(\infty) = 1$ very fast as $\xi \rightarrow \infty$ (with a correction decaying at least as $e^{-\xi^3/3}$). The profile $\rho(\xi)$ is shown in Fig. 4.

It is also interesting to look at the mass distribution on larger scales ξt^α , $2/3 < \alpha \leq 1$. On the ballistic scale $x = \xi t$, one finds (Appendix B)

$$\lim_{t \rightarrow \infty} \pi(\xi t, M, t) = \frac{\xi^2}{\sqrt{\pi}} \Gamma_{-1/2}(M\xi^2), \quad \xi < 0 \quad (53)$$

which of course agrees with the the limit of (17) as $M_0 \rightarrow \infty$. The existence of the distribution (53) shows that there is a number of forerunner particles in the front of the profile that move freely without undergoing aggregation anymore. They carry the finite amount of mass $\mathcal{M} = 1/4\xi^2$ at distance ξt . At shorter distances $|\xi| t^\alpha$, $2/3 < \alpha < 1$, the mass of an aggregate grows as a consequence of the collisions with faster particles coming from the right (the semi-infinite right interval acts here as an infinite reservoir of particles). The rate of growth is of the order $t^{2(1-\alpha)}$ since according to (49) and (50)

$$\mathcal{M}(\xi t^\alpha) = t^{2/3} \mathcal{M}(\xi t^{\alpha-2/3}) \sim \frac{t^{2(1-\alpha)}}{4\xi^2}, \quad t \rightarrow \infty \tag{54}$$

At distances $|\xi| t^{2/3}$ or shorter one recovers the mass growth $\sim t^{2/3}$ that is typical for the homogeneous ballistic aggregation process.

3.2. Aggregation with Particles at Rest

The initial particles occupy again the sites of the right semi-infinite lattice $\{ka, k = 1, 2, \dots\}$, but now we have particles at rest on the left semi-infinite lattice. The probability to find j initially excited particles left of x is obtained by letting $N \rightarrow \infty$ in (30). Since again $\lim_{N \rightarrow \infty} \tilde{J}_m(Y, N, t) = J(Y, t)$ this yields

$$\tilde{H}_m(x, j, t) = \tilde{J}_m((j+1/2)a - x, j, t) J(x - (j+1/2)a, t) \tag{55}$$

where $\tilde{J}_m(Y, j, t)$ is the function (31). According to the discussion of constraints following (31), $\tilde{J}_m((j+1/2)a - x, j, t)$ is equal to the expression (32) when $x < 0$ whereas it reduces to $J_m((j+1/2)a - x, j, t)$ when $x > 0$. The continuum limit gives similarly to (43)

$$\begin{aligned} \tilde{J}(Y, M, t) &= \lim_{m \rightarrow 0} \frac{1}{\sqrt{m}} \tilde{J}_m(Y, j, t) \\ &= \frac{1}{2} \int_{Y^2/2t}^\infty dP \frac{\partial}{\partial P_0} K_f(0, P_0, M, P)|_{P_0=0}, \quad 0 < M \leq Y \end{aligned} \tag{56}$$

where the only change occurs in the lower integration limit, and

$$\tilde{J}(Y, M, t) = J(Y, M, t), \quad M \geq Y \tag{57}$$

The function $\tilde{J}(Y, M, t)$ for $0 < M \leq Y$ is given in the Appendix B.

The time dependence is determined by scaling as in (47) with

$$\tilde{\pi}(\xi, \mu) = \tilde{J}(\mu - \xi, \mu) J(\xi - \mu), \quad \mu > 0 \quad (58)$$

and the average mass left of $\xi t^{2/3}$ is⁶

$$\begin{aligned} \tilde{M}(\xi t^{2/3}, t) &= t^{2/3} \tilde{M}(\xi) \\ \tilde{M}(\xi) &= \int_0^\infty d\mu \mu \tilde{J}(\mu - \xi, \mu) J(\xi - \mu) \end{aligned} \quad (59)$$

For $\xi > 0$ all the predictions are the same as in Section 3.1. When $\xi < 0$ the mass density of excited particles $\tilde{\rho}(\xi) = d\tilde{M}(\xi)/d\xi$ decays exponentially fast as $\xi \rightarrow -\infty$ (Appendix B) and is plotted in Fig. 4. Compared to the slow decay found in (50), this corresponds to the fact that here no particles can move ballistically in the front of the profile.

4. CONCLUDING REMARKS

The asymptotic distribution of mass $\pi^\infty(\xi, M)$ (17) and $\tilde{\pi}^\infty(\xi, M)$ (35) have been derived in Section 2 under the assumption of the Gaussian distribution (1) of initial momenta. It would be of interest to investigate to what extent these results are universal, i.e., independent of the specific form of the initial momentum distribution, provided that the latter is symmetric, scales with m as in (1), and is sufficiently regular. Results of this type have been obtained in ref. 13.

In the continuum limit, the statistics of aggregating particles (with Gaussian initial velocity distribution (1)) is the same as that of shocks in the one-dimensional Burgers turbulence when the initial Burgers velocity field $u_0(x) = u(x, t = 0)$ is a white noise (refs. 2, 12, and references therein). In the homogeneous situation, the (one-dimensional) fluid extends over the whole space and $u_0(x)$ is a white noise for $-\infty < x < \infty$. The case (ii) (aggregation with particles at rest) corresponds to the situation where the initial excitation $u_0(x)$ is a white noise in a finite or semi-infinite interval and the fluid is at rest elsewhere. Such excitations of the initial Burgers field in a finite interval are studied in ref. 15. Our results can be translated in Burgers language if one recalls that the velocity difference Δu (or force strength) is related to the mass of aggregates by $\Delta u = M/t$. Hence $\pi_{\text{Burgers}}(x, \Delta u, t) = t\pi_{\text{aggreg.}}(x, \Delta ut, t)$ is the probability density for a total

⁶ As in the finite interval case, there is a non zero weight at $M = 0$ when $\xi < 0$, but this does not contribute to the average mass.

force strength Δu left of x , and from there one can obtain the average density of shocks $\rho_{\text{Burgers}}(x, t)$ at the point x . In ref. 15, the probability distribution for the difference Δu of the Burgers field over a distance x is calculated and shown to have a scaling limit in terms of the variables $\bar{x} = x\sqrt{t}$ and $\bar{\Delta u} = \Delta u\sqrt{t}$. In the language of ballistic aggregation this corresponds to our findings, namely to have a mass of order \sqrt{t} at distance of order \sqrt{t} . Also non Gaussian distributions similar to (35) and (39) are obtained. The correspondence of the case (i) (aggregation in empty space) with Burgers theory should still be investigated.

APPENDIX A

For the sake of completeness, we recall the expression of the conditional measure $K_\ell(M_1, P_1, M_2, P_2)$ of Brownian paths starting from P_1 at “time” M_1 , ending at P_2 at “time” M_2 and constrained to remain above the line $\ell(y) = ay + b$

$$K_\ell(M_1, P_1, M_2, P_2) = \exp[a(Z_1 - Z_2) + \frac{1}{2}a^2(M_1 - M_2)] G(M_1, Z_1, M_2, Z_2)$$

$$Z_1 = P_1 - aM_1 - b, \quad Z_2 = P_2 - aM_2 - b \tag{60}$$

where

$$G(M_1, Z_1, M_2, Z_2) = \left(\frac{1}{\pi(M_2 - M_1)}\right)^{1/2} \left[\exp\left(-\frac{(Z_2 - Z_1)^2}{M_2 - M_1}\right) - \exp\left(-\frac{(Z_2 + Z_1)^2}{M_2 - M_1}\right) \right] \tag{61}$$

is the fundamental solution of the diffusion equation

$$\left(\frac{\partial}{\partial M_2} - \frac{1}{4} \frac{\partial^2}{\partial Z_2^2}\right) G(M_1, Z_1, M_2, Z_2) = 0$$

with Dirichlet boundary condition at $Z_2 = 0$.

One obtains from (60), (61) and (15) setting $a = \xi, b = 0$

$$J^\infty(\xi, M) = \frac{2}{\sqrt{\pi M^{3/2}}} \int_{\xi M}^\infty dP(P + \xi M) \exp\left(-\frac{P^2}{M}\right) \tag{62}$$

The result (16) follows from the change of variable $P^2/M \rightarrow P$ and integration by part (also using $\int_{-\infty}^{\infty} du \exp(-u^2) = \sqrt{\pi}$ when $\xi < 0$).

A.1. The Normalization Relation (18)

From (18) we have

$$\begin{aligned} & \int_0^{M_0} dM \pi^\infty(\xi, M) \\ &= \frac{1}{\sqrt{\pi}} \int_0^{M_0} dM \Gamma_{-1/2}(M) + \frac{1}{4\pi} \int_0^{M_0} dM \Gamma_{-1/2}(M) \Gamma_{-1/2}(M_0 - M) \end{aligned} \quad (63)$$

Hence, the normalization (18) is equivalent in Laplace transform to

$$\frac{1}{\sqrt{\pi} s} \tilde{I}_{-1/2}(s) + \frac{1}{4\pi} (\tilde{I}_{-1/2}(s))^2 = \frac{1}{s}$$

This last equality is verified using $\tilde{I}_{-1/2}(s) = \frac{2\sqrt{\pi}}{s} (\sqrt{1+s} - 1)$.

A.2. The Normalization Relation (37)

Consider the case of aggregation with particles at rest. The probability $\tilde{\Pi}_m(x, 0, t)$ to find no excited particles left of x , $x < 0$, can also be computed directly from the probability to find all of them right of x :

$$\begin{aligned} \tilde{\Pi}_m(x, 0, t) &= \left\langle \prod_{r \geq 1} \theta(X_{[x]}^r(t) - x) \right\rangle \\ &= \int dP_1 \cdots \int dP_N \varphi_m(P_1) \cdots \varphi_m(P_N) \prod_{r=1}^N \theta \left(P_r + \frac{(x+rm)^2}{2t} \right) \end{aligned} \quad (64)$$

with $[x] =$ integer part of x . Setting $x = \xi \sqrt{t}$, as $t \rightarrow \infty$ this probability tends to

$$\tilde{\Pi}_m^\infty(\xi, 0) = \int dP_1 \cdots \int dP_N \varphi_m(P_1) \cdots \varphi_m(P_N) \prod_{r=1}^N \theta \left(P_r + \frac{\xi^2}{2} \right) \quad (65)$$

and one sees that in the continuum limit, $\tilde{\Pi}^\infty(\xi, 0) = \lim_{m \rightarrow 0} \tilde{\Pi}_m^\infty(\xi, 0)$ is given by the conditional measure of Brownian paths that start from $P = 0$

at “time” $M = 0$ and are above $-\xi^2/2$ up to “time” M_0 , namely from (60) and (61) with $a = 0$ and $b = -\xi^2/2$

$$\begin{aligned} \tilde{H}^\infty(\xi, 0) &= \frac{1}{\sqrt{\pi M_0}} \int_{-\xi^2/2}^\infty dP \left[\exp\left(-\frac{P^2}{M_0}\right) - \exp\left(-\frac{(P + \xi^2)^2}{M_0}\right) \right] \\ &= \frac{1}{\sqrt{\pi}} \gamma_{1/2}(\xi^4/M_0) \end{aligned} \tag{66}$$

which agrees with (37).

APPENDIX B

B.1. The Functions $J(Y)$ and $J(Y, M)$

The kernel $K_f(M_0, P_0, M, P)$ occurring in (43) is explicitly given in ref. 11, Eq. (29)⁷ in terms of Airy functions, and the function $J(Y, t)$ is found to be in ref. 11, Eqs. (65) and (66)

$$\begin{aligned} J(Y, t) &= t^{-1/3} J(Yt^{-2/3}) \\ J(Y) &= e^{-Y^3/3} \mathcal{J}(Y), \quad \mathcal{J}(Y) = \frac{1}{2i\pi} \int_{-i\infty}^{i\infty} dw \frac{e^{wY}}{Ai(w)} \end{aligned} \tag{67}$$

where $Ai(w)$ is the Airy function as defined in ref. 16.

To determine $J(Y, M, t)$, we first calculate its derivative with respect to M in (43) (setting $t = 1$). Using the fact that $K_f(M_0, P_0, M, P)$ obeys the diffusion equation and vanishes on the parabola $f_Y(M)$ one gets

$$\begin{aligned} \frac{\partial J(Y, M)}{\partial M} &= \frac{1}{8} \int_{f_Y(M)}^\infty dP \frac{\partial^2}{\partial P^2} \left[\frac{\partial}{\partial P_0} K_f(0, P_0, M, P)|_{P_0=0} \right] \\ &= -\frac{1}{8} \frac{\partial^2}{\partial P_0 \partial P} K_f(0, P_0, M, P)|_{P_0=0, P=f_Y(M)} \\ &= -\frac{1}{2} I(M, f_Y(M)) \end{aligned} \tag{68}$$

⁷ v in this equation stands for our variable Y and $D = 1/2$ in the present paper.

with $I(M, P)$ the function given in ref. 11, Eqs. (49), (54) and (55)

$$I(M, P) = 2 \exp \left[-\frac{P^2}{M} - \frac{M^3}{12} \right] \mathcal{I}(M) \quad (69)$$

$$\mathcal{I}(M) = \sum_{k \geq 1} e^{-\omega_k M}, \quad -\omega_k = \text{zeros of the Airy function}$$

This leads to

$$\frac{\partial J(Y, M)}{\partial M} = -e^{-Y^3/3} e^{-(M-Y)^3/3} \mathcal{I}(M) \quad (70)$$

By integration of (70) (remember that $J(Y) = \lim_{M \rightarrow \infty} J(Y, M)$) the final result is

$$J(Y, M) = J(Y) + J^*(Y, M) \quad (71)$$

$$J^*(Y, M) = e^{-Y^3/3} \int_M^\infty du \mathcal{I}(u) e^{-(u-Y)^3/3}$$

The time dependence can be restored by the scaling relations (46). The asymptotic behaviors of the functions \mathcal{I} and \mathcal{J} are

$$\mathcal{I}(Y) \sim 2 |Y| e^{-|Y|^3/3}, \quad Y \rightarrow -\infty, \quad \mathcal{I}(Y) \sim \frac{e^{-\omega_1 Y}}{Ai'(-\omega_1)}, \quad Y \rightarrow \infty \quad (72)$$

$$\mathcal{I}(M) \sim \frac{1}{\sqrt{4\pi M^3}}, \quad M \rightarrow 0, \quad \mathcal{I}(M) \sim e^{-\omega_1 M}, \quad M \rightarrow \infty \quad (73)$$

B.2. Proof of (50) and (53)

We first show (53). According to the decomposition (71) of $J(Y, M) = J(Y) + J^*(Y, M)$ one can split $\pi = \pi^{(1)} + \pi^{(2)}$ (47) into two contributions

$$\pi^{(1)}(x, M, t) = t^{-2/3} J^*(M' - x', M') J(x' - M') \quad (74)$$

$$\pi^{(2)}(x, M, t) = t^{-2/3} J(M' - x') J(x' - M')$$

Setting $x = \xi t$ and inserting the expression (71) of $J^*(Y, M)$, the first contribution becomes

$$\begin{aligned} \pi^{(1)}(M, \xi t, t) &= t^{-2/3} \int_{Mt^{-2/3}}^{\infty} du \mathcal{J}(u) \exp\left(-\frac{1}{3}(u - Mt^{-2/3} + \xi t^{1/3})^3\right) \mathcal{J}(\xi t^{1/3} - Mt^{-2/3}) \\ & \quad (75) \end{aligned}$$

For $\xi < 0$ one can replace $\mathcal{J}(Y)$ by its asymptotic form (72) as its argument tends to $-\infty$:

$$\mathcal{J}(\xi t^{1/3} - Mt^{-2/3}) \sim 2 |\xi t^{1/3} - Mt^{-2/3}| \exp\left(-\frac{1}{3} |\xi t^{1/3} - Mt^{-2/3}|^3\right), \quad \xi < 0 \quad (76)$$

We now collect the non vanishing terms in the exponentials as $t \rightarrow \infty$, namely

$$\begin{aligned} \exp\left[-\frac{1}{3} (|\xi t^{1/3} - Mt^{-2/3}|^3 + (u - Mt^{-2/3} + \xi t^{1/3})^3)\right] \\ \sim \exp(-u^3/3 - u\xi^2 t^{2/3} - u^2 \xi t^{1/3}) \end{aligned} \quad (77)$$

Taking (76) and (77) into account in (75) and changing the integration variable $u = \xi^{-2} t^{-2/3} v$ leads to

$$\pi^{(1)}(\xi t, M, t) \sim \frac{2}{|\xi| t} \int_{M\xi^2}^{\infty} dv \mathcal{J}\left(\frac{v}{\xi^2 t^{2/3}}\right) \exp\left[-\frac{v^3}{3\xi^6 t^2} - \frac{v^2}{\xi^3 t} - v\right], \quad t \rightarrow \infty \quad (78)$$

The dominant contribution comes from the divergence (73) of the \mathcal{J} function for small argument. Thus using (73) in (78) and letting $t \rightarrow \infty$ one finds eventually

$$\lim_{t \rightarrow \infty} \pi^{(1)}(\xi t, M, t) = \frac{\xi^2}{\sqrt{\pi}} \int_{M\xi^2}^{\infty} dv v^{-3/2} e^{-v} \quad (79)$$

which is identical to (53). Moreover, $\lim_{t \rightarrow \infty} \pi^{(2)}(\xi t, M, t) = 0$ as a consequence of the fact that $\mathcal{J}(Y)$ function tends to zero fast both for large positive and negative values of its argument (see (72)). This proves (53). The time asymptotics of the distribution $\pi(\xi t, M, t)$ (22) corresponding to initial particles in a finite interval can be determined along the same lines, leading to the result (17).

To show (50), one splits $\mathcal{M}(\xi) = \mathcal{M}^{(1)}(\xi) + \mathcal{M}^{(2)}(\xi)$ as above with

$$\begin{aligned}\mathcal{M}^{(1)}(\xi) &= \int_0^\infty d\mu \mu J^*(\mu - \xi, \mu) J(\xi - \mu) \\ \mathcal{M}^{(2)}(\xi) &= \int_0^\infty d\mu \mu J(\mu - \xi) J(\xi - \mu)\end{aligned}\tag{80}$$

In

$$\mathcal{M}^{(1)}(\xi) = \int_0^\infty d\mu \mu \int_\mu^\infty du \mathcal{F}(u) e^{-(u-\mu+\xi)^3/3} \mathcal{F}(\xi - \mu)\tag{81}$$

one replaces $\mathcal{F}(\xi - \mu)$ by its asymptotic behavior (72) for large negative argument

$$\begin{aligned}\mathcal{M}^{(1)}(\xi) &\sim \int_0^\infty d\mu \mu 2 |\xi - \mu| \int_\mu^\infty du \mathcal{F}(u) \exp[-u^3/3 - (\xi - \mu)u^2 - (\xi - \mu)^2u] \\ &\sim \frac{2}{\xi^2} \int_0^\infty d\mu \mu |\xi - \mu| \int_{\mu\xi^2}^\infty dv \mathcal{F}\left(\frac{v}{\xi^2}\right) e^{-v}\end{aligned}\tag{82}$$

where the second line results of the change of variable $u\xi^2 = v$ and keeping only the dominant contribution as $\xi \rightarrow -\infty$ in the exponential. In this limit, only the asymptotic behavior (73) of $\mathcal{F}(u)$, $u \rightarrow 0$ matters. When this is introduced in (82), the integrals can be evaluated leading to (50). In view of (72), $\mathcal{M}^{(2)}(\xi)$ tends to zero exponentially fast as $\xi \rightarrow \pm\infty$.

B.3. The Function $\tilde{J}(Y, M)$

We proceed as in (68)–(71). The only difference is that the lower integration limit $f_Y(M)$ is replaced by $Y^2/2$. This leads to

$$\frac{\partial \tilde{J}(Y, M)}{\partial M} = -\frac{1}{2} I(M, Y^2/2), \quad 0 < M \leq Y\tag{83}$$

Using (69) and integrating from M to Y gives

$$\tilde{J}(Y, M) = J(Y, Y) + \int_M^Y du \exp\left(-\frac{Y^4}{4u} - \frac{u^3}{12}\right) \mathcal{F}(u), \quad 0 < M \leq Y\tag{84}$$

where one has taken into account that $\tilde{J}(Y, Y) = J(Y, Y)$ (see (57)) and $J(Y, Y)$ can be found from (71). Time dependence can be reintroduced by scaling.

One checks, with the help of these equations and the asymptotic behaviors of the functions \mathcal{J} and \mathcal{I} (72) and (73), that $\tilde{M}(\xi)$ decays exponentially fast as $\xi \rightarrow -\infty$.

REFERENCES

1. G. F. Carnevale, Y. Pomeau, and W. R. Young, *Phys. Rev. Lett.* **64**:2913 (1990).
2. J. M. Burgers, *The Nonlinear Diffusion Equation* (Reidel, Dordrecht, 1974).
3. S. Kida, *J. Fluid Mech.* **93**:337 (1979).
4. W. A. Woyczyński, *Burgers-KPZ Turbulence*, Lecture Notes in Mathematics, Vol. 1700 (Springer, Berlin, 1998).
5. S. Gurbatov, A. Malakhov, and A. Saichev, *Nonlinear Random Waves and Turbulence in Non Dispersive Media: Waves, Rays and Particles* (Nonlinear Science, Manchester University Press, 1991).
6. S. N. Shandarin and Ya. B. Zeldovich, *Rev. Mod. Phys.* **61**:185 (1989).
7. M. Kardar, G. Parisi, and Y. C. Zhang, *Phys. Rev. Lett.* **56**:889 (1986).
8. T. M. Ligett, *Ann. Probab.* **25**:1 (1997).
9. Ph. A. Martin and J. Piasecki, *J. Statist. Phys.* **76**:447 (1994).
10. L. Frachebourg, Ph. A. Martin, and J. Piasecki, *Physica A* **279**:69 (2000).
11. J. Bertoin, Some properties of Burgers turbulence with white or stable noise initial data, in *Lévy Processes: Theory and Applications*, Barndorff-Nielsen, Mikosch, and Resnick, eds. (Birkhäuser, 2001).
12. L. Frachebourg and Ph. A. Martin, *J. Fluid Mech.* **417**:323 (2000).
13. T. Suidan, *J. Statist. Phys.* **101**:893 (2000).
14. I. S. Gradshteyn and I.M. Ryzhik, *Table of Integrals, Series and Products*, 5th ed. (Academic Press, 1994).
15. R. Tribe and O. Zaboronski, *Comm. Math. Phys.* **212**:415 (2000).
16. M. Abramowitz and I. A. Stegun, *Handbook of Mathematical Functions* (Dover, New York, 1965).